

Bursty Wave Instabilities in Open Driven Plasmas

P. A. Robinson,^{1,*} H. B. Smith,^{1,2} and R. M. Winglee³

¹*School of Physics, University of Sydney, Sydney, N.S.W. 2006, Australia*

²*Institute of Advanced Studies, Australian National University, Canberra A.C.T. 2601, Australia*

³*Geophysics, Box 351650, University of Washington, Seattle, Washington 98195-1650*

(Received 22 November 1995)

Wave instabilities in open, driven systems cause bursty emission. Local burst properties are combined with global power balance to predict the source dynamics, energy conversion efficiency, and distribution of power levels. Sporadic growth near marginal stability is characterized by noninteger scaling exponents and an exponential distribution of power levels, unlike self-organized criticality or stochastic growth. Predictions are confirmed by particle-in-cell simulations of driven cyclotron instabilities. Solar microwave bursts are found to have the predicted distribution of power levels. [S0031-9007(96)00158-5]

PACS numbers: 52.35.Qz, 52.25.Gj, 52.65.Rr, 96.60.Rd

In many natural and laboratory situations unstable waves grow in driven, inhomogeneous, open plasmas, leading to clumpy waves within the source and highly variable radiation from it. Examples include some solar and stellar flare emissions, interplanetary, planetary and auroral radio bursts, radiation from beam-plasma experiments, and spiky emissions observed during electron cyclotron heating of mirror plasmas [1–10]. These systems are far from common theoretical idealizations of smoothly varying plasmas whose instabilities can be studied entirely by local uniform-plasma methods. It is a challenge to develop analytic methods that can handle them. Here, we investigate electron cyclotron maser emission (ECME) from a driven inhomogeneous open system. This is a problem that is important in its own right because of its application in contexts such as generation of solar microwave spike bursts which derive their energy from hot electrons generated in solar flares [2,3,5]. It also serves as a representative example of the broad class of extended systems, common in space and astrophysics, in which waves, such as beam-driven waves, are driven unstable due to steady buildup of particle free energy; much of our analysis is correspondingly general. Unlike coherent laboratory sources, such systems typically are not contained in a resonant cavity and involve a *classical* population inversion over a finite continuous range, rather than discrete levels.

Early particle-in-cell (PIC) simulations of ECME showed that, even when the driving is uniform, wave growth is highly nonuniform and radiation from the driven region is bursty, consistent with observed highly spiky solar microwave emissions [1,3,4]. Taking individual spikes to constitute *elementary bursts* (EBs) [2], self-consistent length and time scales of EBs were derived and it was possible to reconcile the theoretical time scales of individual bursts with solar observations [5]. In this picture, it was argued that EBs relax particle free energy in small localized regions, then propagate away, after which free energy rebuilds due to particle advection until another EB relaxes it. Typically, waves interact with

most a few EB regions before dropping out of resonance with the energy source because of gradients in the source parameters (e.g., magnetic field, density, etc.) [2,5], unlike stochastic growth which involves interactions with large numbers of uncorrelated regions [6–8]. We also show below that the bursty energy emission is unlike that in self-organized criticality [11] because it involves a characteristic scale. Statistical properties are shown to distinguish the three regimes clearly.

Despite the success of *local* EB theory, the physics of individual bursts has never been incorporated into a model of the overall dynamics of the source region, nor has it been possible to compare the predicted scaling exponents directly with simulations.

In this Letter, we combine the local physics of EBs with considerations of global power balance to determine the dynamics of the source region and scalings of observable quantities. The results are then successfully verified against inhomogeneous PIC simulations and solar microwave observations.

The model investigated here involves wave growth in an extended open system in which free energy is continually replenished. The particle free energy F is transferred to energy W in unstable waves as well as being lost via spontaneous emission of other waves. The waves can escape through one or more boundaries and it is assumed that the instability is narrow band. This implies that unstable waves of a given frequency only interact with particles over a distance much less than the system size L because gradients in the system parameters cause them to drop out of resonance. The resulting equations are

$$d\langle F \rangle / dt = A(R) - \alpha \langle FW \rangle - S, \quad (1)$$

$$d\langle W \rangle / dt = \alpha \langle FW \rangle - c \langle |\partial W / \partial x| \rangle, \quad (2)$$

where x is position, t is time, α is a constant, angle brackets denote global averages, and R is the rate of increase of free energy in the absence of relaxation. (i) Spontaneous emission S is assumed to be broad band and approximately

constant with respect to R in the steady state and its input to the narrow band unstable waves is neglected. (ii) In the steady state, the mean net deposition rate of energy $A(R)$ is given by $A(R) = A_0 R [1 - \exp(-\gamma t_c)] + S$, where A_0 is a constant and γ is an effective relaxation rate, which allows for incomplete energy transfer from source to waves in a wave-particle interaction time t_c . Taking EBs to be the fundamental entities in the system, it has been shown that $\gamma \sim R^{1/2}$ [5]. In the systems of interest here, $t_c \propto 1/R$ (see below), and hence

$$A(R) = A_0 R \left[1 - \exp\left(-\sqrt{R_c/R}\right) \right] + S, \quad (3)$$

where R_c is a constant. Note that $A(R) - S \sim R$ at small R , while $A(R) - S \sim R^{1/2}$ for large R . (iii) We assume that the instability growth rate is αF near marginal stability, a good approximation for many plasma instabilities [12]. Inside an EB the local wave energy W then increases as $dW/dt = \alpha FW$ in the absence of losses, with $F \sim Rt$ prior to saturation, which occurs at $t \sim R^{-1/2}$ [5]. The resulting average power transfer to unstable waves is $\alpha \langle FW \rangle \sim R^{1/2} \langle W \rangle$. (iv) According to previous theory, each EB acts essentially as an independent source [2,5] and observed waves are an aggregate over the source. The power emitted from an EB region is $\sim c |\partial W / \partial x|$. The EB size is predicted to scale as $R^{-1/2}$ [5], implying $\langle |\partial W / \partial x| \rangle \sim R^{1/2} \langle W \rangle$. Hence, local gradients dominate in determining the loss rate from each EB region and the resulting total output.

In the steady state the net power input to the system $A(R)$ is balanced by the output $\langle P \rangle = \alpha \langle FW \rangle + S = c \langle |\partial W / \partial x| \rangle + S$. The above considerations imply $\langle P \rangle - S \sim R^{1/2}$ for large R and $\langle P \rangle - S \sim R$ for small R . The conversion efficiency into unstable waves is $\epsilon(R) = [A(R) - S]/R = [\langle P \rangle - S]/R$; the remainder of the gross power input $A_0 R$ exits as residual particle energy or via spontaneous emission. Hence, $\epsilon(R) \approx \text{const}$ at small R and $\epsilon(R) \sim R^{-1/2}$ at large R . At small R , (1) and (2) imply $\langle F \rangle \sim \text{const}$ and $\langle W \rangle \sim R$ if S is neglected. Similarly, at large R , $\langle F \rangle \sim R^{1/2}$ and $\langle W \rangle \sim \text{const}$. Dominance of EBs thus implies quite different dynamics at large R , characterized by noninteger exponents.

Emission from the driven system is expected to be random with fluctuations about the mean power output [3,4]. In a source in which many independent EBs occur, there is a certain probability per unit length of intense resonant EB radiation being in an unrelaxed source region whose free energy it can accumulate. The probability distribution of the instantaneous power reaching a level P is thus expected to have the form $f(P) \sim \exp(-P/P_0)$ for $P \gg P_0$, where P_0 is predicted to be proportional to $\langle P \rangle$, the only relevant power scale. Values $P \ll P_0$ are unlikely in a large system, because many EBs are active simultaneously, so $f(P)$ should decrease for $P < P_0$. In general, we predict

$$f(P) = P_0^{-1} g(P/P_0), \quad (4)$$

with $g(0) = 0$ and $g(u) \sim e^{-u}$ for large u . The distribution of peak values of instantaneous power should have the same properties, but with P_0 somewhat larger.

We use electromagnetic PIC simulations to test the above theory, following three velocity components of 48 000 electrons in one spatial dimension (a $1\frac{1}{2}$ dimensional simulation) [3,4]. Ions are treated as fixed, infinitely massive particles. The simulation system shown in Fig. 1 is analogous to the one studied from a different perspective in Ref. [3] and consists of a plasma in an ambient magnetic field \mathbf{B} directed perpendicular to the system and having the profile shown. The system has a total length L divided into 2048 cells, each of length $c/7\omega_p$. The plasma contains two electron components with initial momentum distributions of the form [13]

$$F_i(v_{\parallel}, v_{\perp}) = \frac{N_i}{j! (2\pi V_i^2)^{3/2}} \left(\frac{v_{\perp}^2}{2V_i^2} \right)^j e^{-v^2/2V_i^2}, \quad (5)$$

where $v^2 = v_{\parallel}^2 + v_{\perp}^2$, v_{\parallel} and v_{\perp} are momentum components (in units of $m_e c$) parallel and perpendicular to \mathbf{B} , N_i is the number of particles in the i th distribution, V_i is the corresponding thermal momentum, and j is a constant. In our work we choose an initial electron distribution comprising a stable cold background component in regions II and IV of Fig. 1 ($N_c = 25\,800$, $V_c = 0.5$, $j = 0$) and an unstable hot energetic component in the source, region III ($N_h = 22\,200$, $V_h = 1.0$, $j = 2$). Energy is injected by randomly removing a small fraction of the hot electrons from region III every few time steps and replacing them with electrons chosen from the initial hot distribution—the *recycling* procedure [3,4]. The resulting population inversion in v_{\perp} drives a maser instability, which tends to relax the distribution toward marginal stability by flattening it in the v_{\perp} direction. Energy is transferred to waves, which grow in a bursty fashion, exit the hot plasma, and are damped by the cool plasma in regions II and IV or by the absorbing vacuum [3,4] in regions I and V that prevents reflections back into the system. In region III,

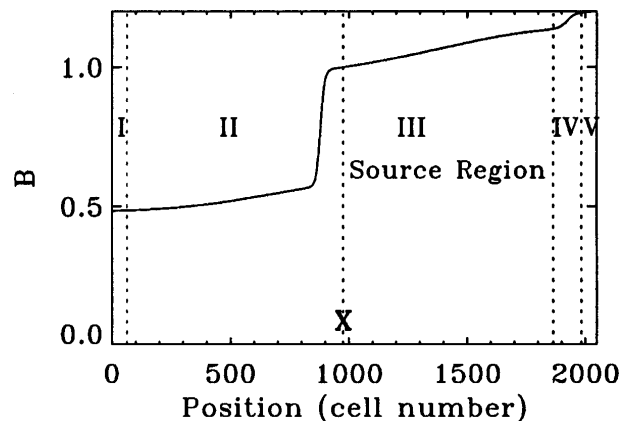


FIG. 1. Simulation system, showing the magnetic field profile and regions of plasma and vacuum described in the text.

the plasma frequency is $\omega_p = \Omega_e/7$, where Ω_e is the electron cyclotron frequency. Also, $c = 7$ in these units. The probability per unit time of recycling a given hot particle is $1/T_R = R/N_h$ where R is the recycling rate and T_R is the recycling time, which is also the characteristic interaction time t_c . All the simulation parameters except R and T_R are held constant in what follows and (except for $R = 0$) we examine long-term steady-state behavior.

A general point regarding the simulations is that radiation from region III is highly bursty, despite the driving being spatially uniform (apart from statistical noise). Also, the steady-state electron distribution in region III is observed to be close to marginal stability, highly flattened in the v_\perp direction. Both observations are consistent with previous results [3,4].

Before testing the predicted scalings of the power output and other quantities, we estimate $\epsilon(0)$ by running a simulation with $R = 0$. The energy of the system initially decreases rapidly as ECM radiation grows and escapes, relaxing the distribution toward marginal stability, a point confirmed by direct examination of the velocity distribution. Later, the energy decreases at a smaller, nearly constant rate due to spontaneous emission. Extrapolation of this later behavior back to $t = 0$ yields a net maser conversion efficiency of $\epsilon(0) = (7.3 \pm 0.7)\%$ of the total electron energy. An analytic estimate of $\epsilon(0)$ can be obtained from the difference between the energy of the initial distribution and the marginally stable one, giving $\epsilon(0) \approx 7\%$, in agreement with the numerical result.

The net power input to the hot electrons can be obtained by calculating the difference between the gross energy injected via recycling and the residual energy of particles removed in this process. The squares in Fig. 2 show the resulting $\langle P \rangle$ vs $R^{1/2}$ for $2.5 \leq R/\omega_p \leq 160$; data from $R = 0$ cannot be used because it is not a steady-state system. A least squares best fit yields $\langle P \rangle \approx 0.33 + 0.58(R/\omega_p)^{1/2}$, consistent with the expected large- R dependence in the presence of spontaneous emission. A more restricted set of runs with twice as many particles also gave a linear dependence on $R^{1/2}$. If the constant term is subtracted from these results and a log-log least squares fit done to the resulting data, we obtain $\langle P \rangle - S \sim R^{0.51 \pm 0.01}$, in excellent agreement with theory over nearly 2 decades; results with twice as many particles gave an exponent of 0.49. Triangles show the resulting efficiency obtained from $\epsilon(R) = [\langle P \rangle - S]/R$. Fitting of (3) to these data, assuming the theoretical value $\epsilon(0) = 0.07$, then gives $R_c \approx 0.04\omega_p$. The results of earlier local EB theory [5] are thus also confirmed, since they are implicit in the above scalings. Unfortunately, we cannot simulate $R \ll R_c$ in the steady state in a feasible amount of computer time and so cannot reach a regime where the more intuitive scaling $\langle P \rangle \sim R$ is attained. Separate estimates of the scalings of $\langle P \rangle$ and $\epsilon(R)$ can be obtained by calculating the Poynting flux at the point X in Fig. 1 directly from the PIC fields. A fit to

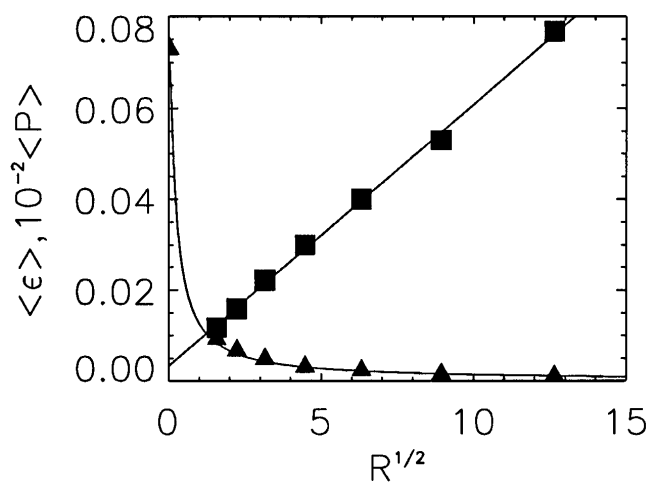


FIG. 2. Mean power output $\langle P \rangle$ (squares, arbitrary units) and efficiency $\epsilon(R)$ (triangles) vs R , showing fits to $\langle P \rangle$ (straight line) and $\epsilon(R) = [A(R) - S]/R$ (curve) using (3) with $\epsilon(0) = 0.07$ and $R_c = 0.04\omega_p$.

this flux as a function of R for $2.5 \leq R \leq 160$ yields $\langle P \rangle - S \sim R^{0.50 \pm 0.01}$ and $\epsilon(R) \sim R^{-(0.50 \pm 0.01)}$ at large R , in close agreement with theory and the scalings found above; consistent exponents were found for a limited set of runs with twice as many particles.

The probability distribution of instantaneous power output at X is found to have an exponential tail at large P , as predicted by (4). Significantly, the existence of the characteristic scale P_0 implies that the fluctuations about marginal stability do not represent a case of self-organized criticality, which is scale free with a power-law distribution of P [11]. Nor is this a case of stochastic growth via many independent increments of gain, as recently studied in connection with type-III solar radio bursts, which yields a lognormal distribution of P [6–8]. Numerically, $P_0 \sim R^{0.51 \pm 0.02}$ for $2.5 \leq R/\omega_p \leq 160$, in excellent agreement with theory and the scaling of $\langle P \rangle$. Figure 3 shows $P_0 f(P)$ vs P/P_0 for the cases $R = 10\omega_p$ and $R = 80\omega_p$. (i) The curves have the same slope and they peak at $P \sim P_0$, consistent with (4). (ii) The predicted value $f(0) = 0$ is not seen because $f(P)$ is accumulated in finite bins, which blur its form, especially at small R where the bin size is a larger fraction of P_0 . However, $f(0)$ is found to be a factor of 2–5 smaller than the peak of $f(P)$. (iii) Spontaneous emission reduces the chance of $P \leq S$ being attained, effectively restricting $f(P)$ to a smaller range at higher P than would otherwise be the case. This tends to shift the curves in Fig. 3 upwards and to the right, and is more pronounced for small R , where S/P_0 is larger. Estimation of this offset implies that it can account for the difference between the two curves in Fig. 3. (iv) The distributions of maximums $f(P_{\max})$ are found to follow a similar functional form, as predicted, but with a larger dip at low P (by a factor of 5–100), especially at large R where noise is least important.

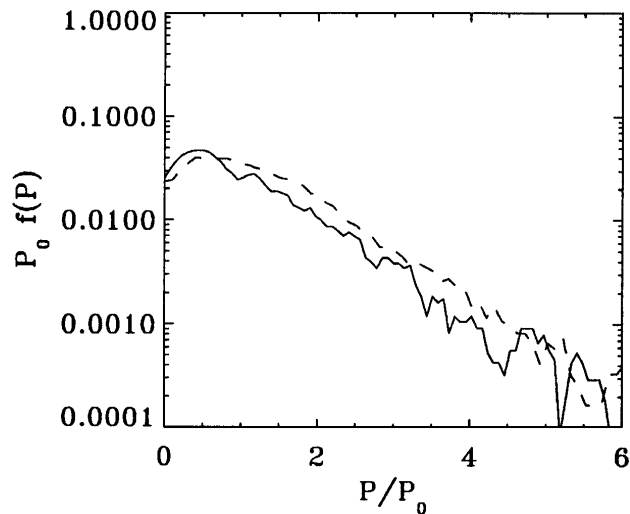


FIG. 3. Distribution $P_0 f(P)$ vs P/P_0 for $R = 10\omega_p$ (dashed) and $R = 80\omega_p$ (solid).

(v) Consistent results were found for a small set of runs with twice as many particles.

Figure 4 shows an observed distribution of power maximums, obtained by us from the first half of the final frame of Fig. 1 of Ref. [1], which showed a time series of power emitted in solar microwave spike bursts, believed to be generated by the ECM instability. This time interval was chosen because, during it, the mean power level was reasonably steady. We see an overall form in excellent agreement with the theoretical expression for P_{\max} [the analog of (4)] and similar to the simulation results in Fig. 3 with a well defined exponential tail, as predicted above. Together with previous work that reconciled theoretical and experimental time scales for *individual* EBs [5], this provides strong support for our global EB model.

The theory developed here combines local elementary burst theory with considerations of global power balance to determine the overall dynamics of the source region, average power output, conversion efficiencies, the distribution of power levels, and other quantities. It shows the importance of self-generated local inhomogeneities and the resulting correlations between free energy, wave energy, and length and time scales in determining the dynamics of the source, which fall into a new *elementary burst regime*, distinct from the categories of self-organized criticality and stochastic growth previously studied. This new regime is characterized by sporadic growth, noninteger scaling exponents, and an exponential distribution of high power levels. Our simulations numerically verify key features of the theory, providing the first direct confirmation of the predicted noninteger scaling exponents and exponential power-level distributions in this type of system. Similarly, our successful comparison of $f(P_{\max})$ with solar radio observations further supports the theory and its application to microwave spike bursts.

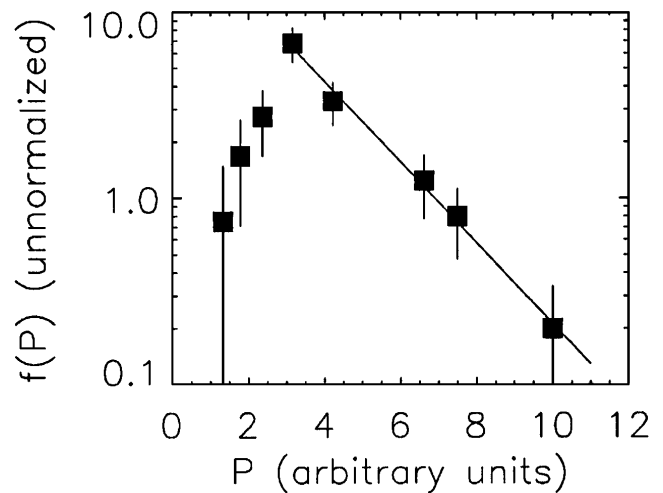


FIG. 4. Distribution of peak solar microwave spike burst power levels. Error bars show statistical uncertainties.

The system considered is representative of the broad class of extended open systems in which waves are driven unstable by gradual input of particle free energy and the results obtained are thus expected to be widely applicable. There is strong evidence that solar microwave spike bursts and some planetary and auroral radio emissions are produced by ECME driven by an unstable distribution similar to the one considered here [2–5], while growth of beam-driven waves in type-III solar radio bursts and planetary foreshocks also involves competition between buildup and relaxation of an unstable distribution.

This work was supported by the Australian Research Council and NSF Grant ATM 9321665.

*Electronic address: robinson@physics.usyd.edu.au

- [1] F. Dröge, *Astron. Astrophys.* **57**, 285 (1977).
- [2] D. B. Melrose and G. A. Dulk, *Astrophys. J.* **259**, 844 (1982).
- [3] R. M. Winglee, G. A. Dulk, and P. L. Pritchett, *Astrophys. J.* **328**, 809 (1988).
- [4] M. E. McKean, R. M. Winglee, and G. A. Dulk, *Sol. Phys.* **122**, 53 (1989).
- [5] P. A. Robinson, *Sol. Phys.* **134**, 299 (1991).
- [6] P. A. Robinson, *Sol. Phys.* **139**, 147 (1992).
- [7] P. A. Robinson, I. H. Cairns, and D. A. Gurnett, *Astrophys. J.* **387**, L101 (1992).
- [8] P. A. Robinson, *Phys. Plasmas* **2**, 1466 (1995).
- [9] B. H. Quon and R. A. Dandl, *Phys. Fluids B* **1**, 2010 (1989).
- [10] G. E. Guest, M. E. Fetzer, and R. A. Dandl, *Phys. Fluids B* **2**, 1210 (1990).
- [11] P. Bak, C. Tang, and K. Wiesenfeld, *Phys. Rev. Lett.* **59**, 381 (1987).
- [12] P. A. Robinson (to be published).
- [13] G. E. Guest and R. A. Dory, *Phys Fluids* **8**, 1853 (1965).